Monitoring defects on monolayer graphene using nematic liquid crystals

Young Jin Lim,[1] Byung Hoon Lee,[1] You Ri Kwon,[1] Young Eun Choi,[1] G. Murali,[1] Joong Hee Lee,[1,2] Van Luan Nguyen,[3,4] Young Hee Lee,[3,4,5] and Seung Hee Lee,[1,2,*]

[1]*Applied Materials Institute for BIN Convergence, Department of BIN Fusion Technology, Chonbuk National University, Jeonju, Jeonbuk, 561-756, South Korea*

[2]*Department of Polymer-Nano Science and Technology, Chonbuk National University, Jeonju, Jeonbuk, 561-756, South Korea*

[3]*Center for Integrated Nanostructure Physics, Institute for Basic Science (IBS), Sungkyunkwan University, Suwon 440-746, South Korea*

[4]*Department of Energy Science, Department of Physics, Sungkyunkwan University, Suwon 440-746, South Korea*

[5]*leeyoung@skku.edu*

[*]*lsh1@chonbuk.ac.kr*

Abstract: Defects in graphene governs electrical and optical properties. Although grain boundaries in graphene inevitably formed during large area synthesis process, which act as scattering centers for charge carriers to degrade mobility, have been studied extensively, point defects have been rarely investigated mainly due to the absence of facile observation tools. Here, we report polarized optical microscopy to observe defect distributions in monolayer graphene. This was realized by aligning liquid crystal s (LC) on graphene where the defect population was modulated by irradiating ultraviolet (UV) light directly on graphene surface under moisture condition. Aromatic rings in LC molecules are oriented with hexagonal rings in graphene to have preferred orientation, providing a way to identify relative orientations of graphene domains and point defects. Our studies show that point defects generated by prolonged UV irradiation time give rise to irregular LC alignment with disclination lines on the graphene surface and a large-size LC domain associated with graphene single domain eventually disappeared. This indicates that defects associated with oxygen-containing functional groups cause to reduce the strong stacking interaction between graphene and LC molecules.

OCIS codes: (240.6700) Surfaces; (040.1880) Detection; (160.3710) Liquid crystals.

References and links

1. . W. Kroto, J. R. Heath, S. C. O'Brien, R. F. Curl, and R. E. Smalley, "C60:Buckminsterfullerene," Nature **318**(6042), 162–163 (1985).
2. C. Wen, J. Li, K. Kitazawa, T. Aida, I. Honma, H. Komiyama, and K. Yamada, "Electrical conductivity of a pure C60 single crystal," Appl. Phys. Lett. **61**(18), 2162–2163 (1992).
3. R. A. Jishi, M. S. Dresselhaus, and G. Dresselhaus, "Electron-phonon coupling and the electrical conductivity of fullerene nanotubes," Phys. Rev. B **48**(15), 11385–11389 (1993).
4. M. S. Dresselhaus, G. Dresselhaus, and R. Saito, "Carbon fibers based on C_{60} and their symmetry," Phys. Rev. B Condens. Matter **45**(11), 6234–6242 (1992).
5. T. W. Ebbesen, H. J. Lezec, H. Hiura, J. W. Bennett, H. F. Ghaemi, and T. Thio, "Electrical conductivity of individual carbon nanotubes," Nature **382**(6586), 54–56 (1996).
6. Z. Wu, Z. Chen, X. Du, J. M. Logan, J. Sippel, M. Nikolou, K. Kamaras, J. R. Reynolds, D. B. Tanner, A. F. Hebard, and A. G. Rinzler, "Transparent, conductive carbon nanotube films," Science **305**(5688), 1273–1276 (2004).
7. A. K. Geim and K. S. Novoselov, "The rise of graphene," Nat. Mater. **6**(3), 183–191 (2007).
8. P. Avouris, "Graphene: Electronic and photonic properties and devices," Nano Lett. **10**(11), 4285–4294 (2010).
9. F. Bonaccorso, Z. Sun, T. Hasan, and A. C. Ferrari, "Graphene photonics and optoelectronics," Nat. Photonics **4**(9), 611–622 (2010).
10. P. Blake, P. D. Brimicombe, R. R. Nair, T. J. Booth, D. Jiang, F. Schedin, L. A. Ponomarenko, S. V. Morozov, H. F. Gleeson, E. W. Hill, A. K. Geim, and K. S. Novoselov, "Graphene-based liquid crystal device," Nano Lett. **8**(6), 1704–1708 (2008).

#239712 - $15.00 USD Received 24 Apr 2015; revised 18 May 2015; accepted 18 May 2015; published 20 May 2015

11. Z. Yan, J. Lin, Z. Peng, Z. Sun, Y. Zhu, L. Li, C. Xiang, E. L. Samuel, C. Kittrell, and J. M. Tour, "Toward the synthesis of wafer-scale single-crystal graphene on copper foils," ACS Nano **6**(10), 9110–9117 (2012).
12. L. Gao, W. Ren, H. Xu, L. Jin, Z. Wang, T. Ma, L.-P. Ma, Z. Zhang, Q. Fu, L. M. Peng, X. Bao, H. M. Cheng, "Repeated growth and bubbling transfer of graphene with millimetre-size single-crystal grains using platinum," Nat. Commun. **3**, 699 (2012).
13. H. Zhou, W. J. Yu, L. Liu, R. Cheng, Y. Chen, X. Huang, Y. Liu, Y. Wang, Y. Huang, and X. Duan, "Chemical vapour deposition growth of large single crystals of monolayer and bilayer graphene," Nat. Commun. **4**, 2096 (2013).
14. Y. Hao, M. S. Bharathi, L. Wang, Y. Liu, H. Chen, S. Nie, X. Wang, H. Chou, C. Tan, B. Fallahazad, H. Ramanarayan, C. W. Magnuson, E. Tutuc, B. I. Yakobson, K. F. McCarty, Y.-W. Zhang, P. Kim, J. Hone, L. Colombo, and R. S. Ruoff, "The role of surface oxygen in the growth of large single-crystal graphene on copper," Science **342**(6159), 720–723 (2013).
15. L. Gan and Z. Luo, "Turning off hydrogen to realize seeded growth of subcentimeter single-crystal graphene grains on copper," ACS Nano **7**(10), 9480–9488 (2013).
16. G. H. Han, F. Güneş, J. J. Bae, E. S. Kim, S. J. Chae, H.-J. Shin, J.-Y. Choi, D. Pribat, and Y. H. Lee, "Influence of copper morphology in forming nucleation seeds for graphene growth," Nano Lett. **11**(10), 4144–4148 (2011).
17. D. L. Duong, G. H. Han, S. M. Lee, F. Gunes, E. S. Kim, S. T. Kim, H. Kim, Q. H. Ta, K. P. So, S. J. Yoon, S. J. Chae, Y. W. Jo, M. H. Park, S. H. Chae, S. C. Lim, J. Y. Choi, and Y. H. Lee, "Probing graphene grain boundaries with optical microscopy," Nature **490**(7419), 235–239 (2012).
18. D. W. Kim, Y. H. Kim, H. S. Jeong, and H. T. Jung, "Direct visualization of large-area graphene domains and boundaries by optical birefringency," Nat. Nanotechnol. **7**(1), 29–34 (2011).
19. J.-S. Yu, D.-H. Ha, and J.-H. Kim, "Mapping of the atomic lattice orientation of a graphite flake using macroscopic liquid crystal texture," Nanotechnology **23**(39), 395704 (2012).
20. J. S. Yu, J. E. Yun, and J.-H. Kim, "Tilt angle change of nematic liquid crystal as a function of the number of graphite layers," Liq. Cryst. **40**(2), 216–220 (2013).
21. J.-H. Son, S.-J. Baeck, M.-H. Park, J.-B. Lee, C.-W. Yang, J.-K. Song, W. C. Zin, and J.-H. Ahn, "Detection of graphene domains and defects using liquid crystals," Nat. Commun. **5**, 3484 (2014).
22. V. L. Nguyen, B. G. Shin, D. L. Duong, S. T. Kim, D. Perello, Y. J. Lim, Q. H. Yuan, F. Ding, H. Y. Jeong, H. S. Shin, S. M. Lee, S. H. Chae, Q. A. Vu, S. H. Lee, and Y. H. Lee, "Seamless stitching of graphene domains on polished copper (111) foil," Adv. Mater. **27**(8), 1376–1382 (2015).
23. F. Güneş, G. H. Han, H.-J. Shin, S. Y. Lee, M. Jin, D. L. Duong, S. J. Chae, E. S. Kim, F. Yao, A. Benayad, J.-Y. Choi, and Y. H. Lee, "UV-light-assisted oxidative sp^3 hybridization of graphene," Nano **6**(5), 409–418 (2011).
24. J. P. Perdew, K. Burke, and M. Ernzerhof, "Generalized gradient approximation made simple," Phys. Rev. Lett. **77**(18), 3865–3868 (1996).

1. Introduction

Indium tin oxide (ITO) with high transparency and low electric resistance has been widely used as a transparent electrode in various electronic devices such as liquid crystal display, organic light emitting diode, solar cell, and touch panel. However, ITO electrode has few drawbacks such as, low flexibility that limits its application in flexible devices and its increasing price as indium is limited natural resources. To replace the ITO, allotropes of nanocarbon materials such as fullerene [1–3], carbon nanotube [4–6], and graphene [7–10] have been investigated owing to their unique electrical and optical properties. In particular, graphene is an attractive material for electro-optic devices; its high optical transmittance, low resistivity, high chemical stability, and mechanical strength with flexibility are adequate to act as an ideal optical transparent conductor. Graphene can be grown ideally from a single nucleation seed, but the growth to large area is terminated by several unknown self-limiting growth factors [11–15]. Another approach is to start with numerous nucleation seeds and allow them to grow and coalesce together to form large-area graphene. However, graphene grain boundaries (GGBs) are inevitably formed via stitching of graphene flakes [16, 17] and deteriorate the quality of graphene. Therefore, it is not easy to synthesize uniform graphene domain in large-size area, which is a key requirement for large-sized device application. In addition, no simple technique is available to examine the quality i.e., domain size, crystal direction and defect sites of the synthesized graphene layers. Recently, a simple method for the visualization of large graphene domains by imaging textures of nematic liquid crystal (LC) director **n** on a graphene surface was reported [18–21]. On the other hand, it has been reported that the GGBs of graphene surface can be visualized via an optical microscope, because the GGBs are oxidized and then they are amplified after UV exposure [17]. Though these methods could analyze defect sites and orientation of the graphene domains, their ability to distinguish the point defects sites is still questionable.

#239712 - $15.00 USD Received 24 Apr 2015; revised 18 May 2015; accepted 18 May 2015; published 20 May 2015

In this paper, the alignment of nematic LC director **n** on the graphene surface has been investigated. The number of defects based on the observation of LC textures through the polarized optical microscope (POM) has been quantitatively analyzed as a function of UV exposure time on the graphene surface. Also, the effect of UV exposure on GGBs in generating point defects is studied and then LC alignment is correlated with increased number of GGBs and defect sites. The reported results suggest that POM is a powerful tool to detect GGBs and defects present in the graphene surface, and allow us to monitor the quality of graphene surface over a large-size area.

2. Experimental procedure

Figure 1 shows several types of defects in graphene that are formed during initial growth stage: Commensurate stitching of two hexagonal graphene domains without forming GGB [Fig. 1(a)] and incommensurate stitching with GGB [Fig. 1(b)], and individual hexagonal graphene domain [Fig. 1(c)]. Point defect defects such as vacancy and Stone-Wales (SW) are usually formed. To observe defects of single crystalline graphene, nematic LC composed of the superfluorinated LC materials from Merck, with birefringence (Δn) of 0.0977 at 589 nm and nematic to isotropic transition temperature (T_{NI}) of 75.5 °C, was used. Thin LC films were directly spin-coated onto the graphene surface with 600 rpm for 23 s and then 2,000 rpm for 70 s. The measured LC film thicknesses using NanoView (Nano System Co.) were in the range of 0.6 to 1μm.

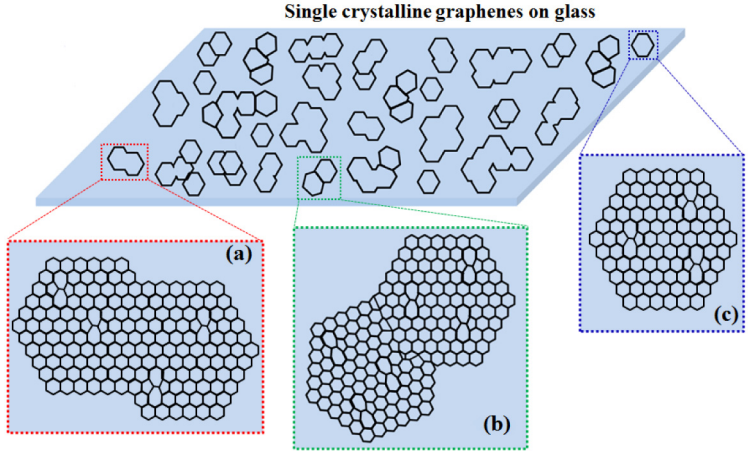

Fig. 1. Schematic representation of typical defects of single crystalline graphene on glass substrate: (a) commensurate and (b) incommensurate stitching of two hexagonal graphene grains, and (c) single hexagonal graphene grain. Point defects (for example SW defect) are visualized in each grain.

To observe defects and GGBs on graphene using the transmission mode of POM, single crystalline graphene was transferred onto a glass substrate by bubbling transfer [22]. In this method, poly(methyl methacrylate) (PMMA, Chem) was spin-coated onto as-grown graphene (1000 rpm, 1 min) as a protection layer and baked at 1200 °C for 1 min. 0.1 M NaOH was used as electrolyte. PMMA/Gr/Cu was used as cathode, while stainless steel was used as anode. 20 V was applied between anode and cathode. Bubbling time was only a few seconds. The PMMA/Gr film was detached from copper, before being transferred to DI water to clean the residuals. It was then transferred to glass substrate. The sample was baked again at 800 °C for 30 min, followed by a PMMA removal using acetone. The transferred single crystalline graphene on glass was examined using POM to observe the LC texture after the LC was spin-coated (at first 600 rpm for 23 s and then 2,000 rpm for 70 s). Then, the LC film was removed by flowing acetone and the graphene/glass substrate was irradiated with UV-light for 5 min to oxidize the samples. Again, the LC texture was observed by spin-coating the LC. In the

#239712 - $15.00 USD Received 24 Apr 2015; revised 18 May 2015; accepted 18 May 2015; published 20 May 2015

similar way, LC texture was observed for further 5, 20 min UV-light treatment (total UV irradiation time 10, 30 min). The UV irradiation oxidizes the samples, as shown in Fig. 2 [22, 23], in which the samples were placed into a chamber equipped with Hg-Xe lamp (Lightning cure, HAMAMATSU, with an output of 20 mW/cm^2 under moisture condition, with the primary emitted light at a wavelength of 365 nm). The defect area and GGBs were oxidized by O and OH radicals, as shown in Figs. 2(a) and (b).

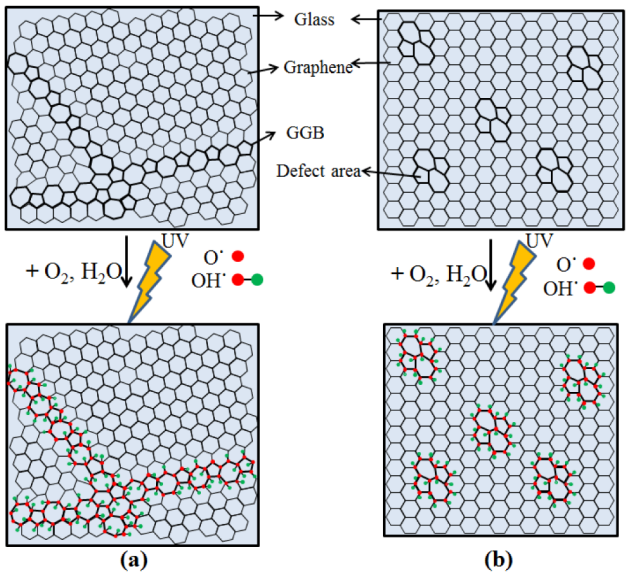

Fig. 2. The schematic diagram of graphene surface on glass according to the UV irradiation treatment under ambient conditions: (a) GGB area and (b) point defect area.

3. Results and discussion

Figure 3 shows POM images of the LC film on single crystalline graphene, where LC alignment was induced by the graphene surface. Before UV irradiation, POM images could not identify all the defects. Some point defects are so small that LC alignment is still retained. However, after UV exposure under moisture conditions, clear defects were observed within hexagonal graphene domains. The domain images show the same color when the LC directors on graphene surface were aligned to the same orientation direction under crossed polarizer. However, the defect area shows different color compared to the surrounding area due to the breakage in orientation direction of LC directors. GGB line is observed in incommensurate stitching after the UV exposure over 10 min, when the edge directions of two hexagonal graphene domains were mismatched, as shown in domain 2 of Fig. 3(c). On the other hand, no GGB line was observed in commensurate stitching after the UV exposure for 30 min, when the edge directions of two hexagonal graphene domains were matched, as shown in domain 2 of Fig. 3(b) and domain 1of the Fig. 3(c).

#239712 - $15.00 USD Received 24 Apr 2015; revised 18 May 2015; accepted 18 May 2015; published 20 May 2015

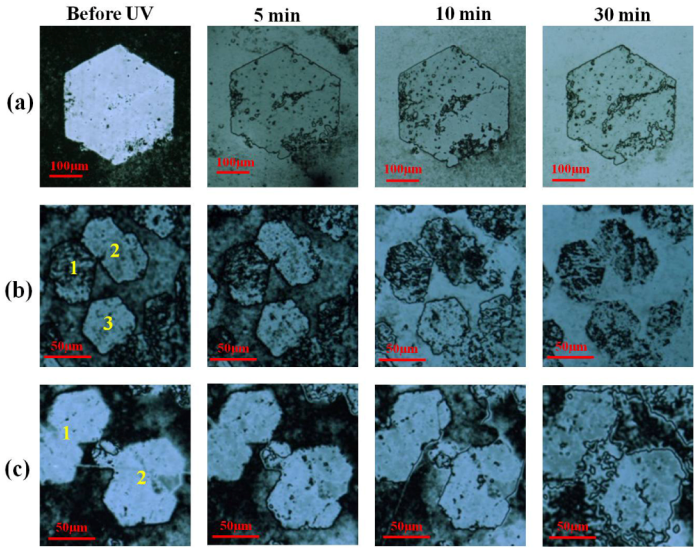

Fig. 3. POM images of the LC domains induced by graphene surface according to UV treatment time under crossed polarizers: (a) Area 1, (b) Area 2 and (c) Area 3.

It is important to confirm the orientation of LC director on graphene surface to understand the defect and GGB. In order to understand how nematic LC molecules align on graphene surface, the binding energy of a single molecule LC, 4-Cyano-4'-pentylbiphenyl (5CB) on graphene was calculated on density functional theory implemented in DMOL code [22–24]. Here, the direction of a 5CB LC molecule was defined as the direction along two benzene rings of 5CB (magenta indicated row). According to calculations, AB stacking between two benzene rings of 5CB LC molecule with graphene (defined as 0 degree) had the strongest binding energy and it was even stronger than AA stacking (defined as 60 degree), as shown in Fig. 4 [22]. It implies that 5CB molecules prefer to align along graphene lattice in a certain direction although this alignment has 3-fold symmetry. Such surface anchoring of LC on graphene surface in a certain direction will induce an easy axis of nematic LC director when nematic LCs are coated on graphene surface.

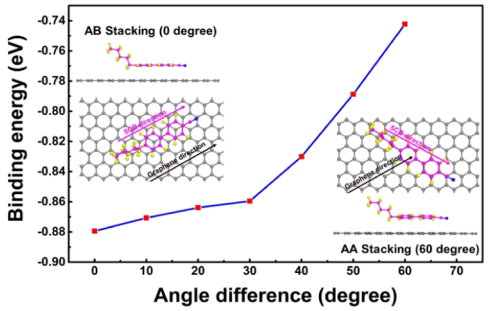

Fig. 4. Density functional theory calculations of the LC alignment on graphene surface. The binding energy is calculated by subtracting the total energies of individual LC and graphene from that of combined LC and graphene system. Although two aromatic rings in free-standing molecule are twisted, they are adsorbed closely parallel to the graphene layer, as shown in the inset, while the tail part is repelled due to hydrophobic nature between graphene and tail of the molecule.

We measured the area with defects (defined as D_I) over the measured whole area (D_w) before UV exposure using an *i*-solution image analyzer (iMTechnology) and calculated defect percentage which is defined as D_I / D_w x 100. After UV exposure, the area with defects is

#239712 - $15.00 USD Received 24 Apr 2015; revised 18 May 2015; accepted 18 May 2015; published 20 May 2015

measured (defined as D_u) again and a defect generation rate which is defined as ΔD (D_u - D_I) / D_I is calculated on each graphene domain under the UV irradiation treatment under moisture conditions, as shown in Fig. 5. In the initial state before UV irradiation, although the defect rate of Area 1 and Area 3-1 is low, as shown in Fig. 5(a), the generation ratio is relatively large when UV irradiation time is increased from 0 to 30 min, as shown in Fig. 5(b). On the contrary, when the defect percentages of Area 2-1 and Area 2-3 are high, the generation rate is relatively small. This implies that the defects of small size are maximized due to oxidation of graphene surface after UV irradiation. As a result, orientation of uniformly aligned LC molecule is significantly deteriorated after UV treatment as compared to before UV treatment, because oxidized defects disturb LC molecules that are aligned in one direction.

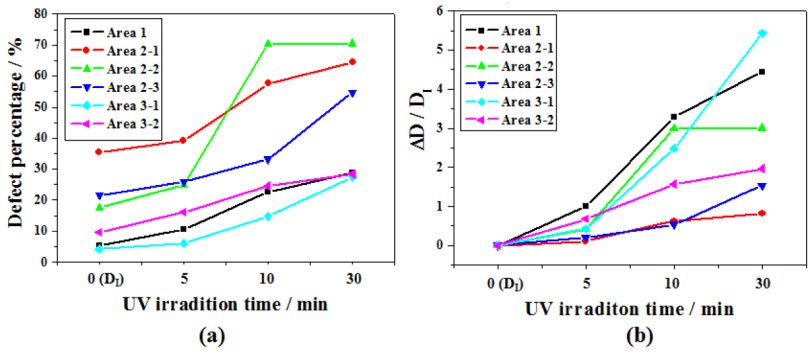

Fig. 5. (a) Defect percentage and (b) defect change ratio in graphene domains along the UV irradiation treatment under ambient conditions.

4. Summary

This study analyzes the orientation of LCs and defects on single crystalline graphene surface according to the UV exposure time. When UV exposure time increased from 0 to 30 min, the defect generation ratio of domains with small size defects increased sharply. Also, the longer UV irradiation time weakens the binding force of LC molecules to graphene and generates more disclination areas on the graphene surface. In other words, the longer UV irradiation time reduces the anchoring energy on the graphene surface, and then makes the LCs orientation irregular by breaking the force of orientation of the LCs. Our studies indicate that nematic LC could be an excellent tool to detect defects on the graphene surface, especially in large-sized area. Though, more works to correlate LC textures with type of defects of graphene surface are under progress.

Acknowledgments

This research was supported by the Basic Research Laboratory Program (2014R1A4A1008140) through the Ministry of Science, ICT & Future Planning and by Basic Science Research Program through the National Research Foundation of Korea (NRF) funded by Ministry of Education (2014R1A1A2004467). One of us (YHL) acknowledges IBS funding (IBS-R011-D1).

#239712 - $15.00 USD Received 24 Apr 2015; revised 18 May 2015; accepted 18 May 2015; published 20 May 2015